Behavioral and Neural Representations of Intertwined Episodes in the Macaque

Zhiyong Jin[1,4], Ning Su[1,2], Aakash Sarkar[3], Jiayu Cheng[1,5], Xufeng Zhou[1,2], Xuanlong Zhu[1], Makoto Kusunoki[6], Sze Chai Kwok[1,2,4,5] *

[1] Duke Kunshan University, Kunshan, China
[2] East China Normal University, Shanghai, China
[3] University of California San Francisco, San Francisco, USA
[4] Westlake University, Hangzhou, China
[5] Wuhan University, Wuhan, China
[6] University of Oxford, Oxford, United Kingdom

*sze-chai.kwok@st-hughs.oxon.org

Introduction

How the brain organizes the temporal structure of experience across different timescales remains unclear (Clayton & Dickinson, 1998). Here, we examine population dynamics in primate medial posterior parietal cortex during temporal order judgments (Zuo et al., 2026) spanning seconds to minutes and across-day episodes. We propose that temporal memory is supported by a unified low-dimensional manifold whose geometric integrity and dynamical structure enable accurate retrieval.

Task Paradigm and Results

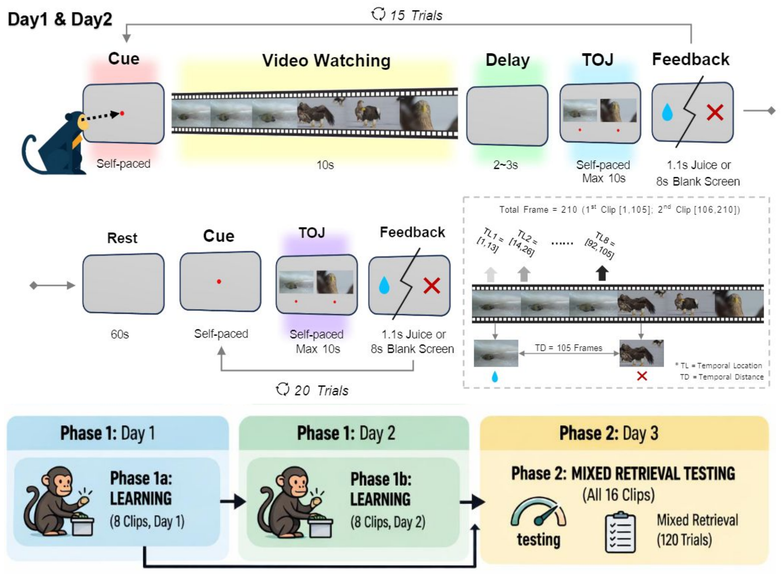

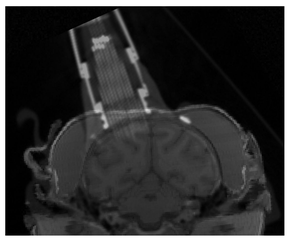

Fig. 1 TOJ memory task, three-day paradigm structure, and recording site. On Days 1 and 2, monkeys viewed 10-s videos (two concatenated 5-s clips). Following a 2-s delay, they performed a two-alternative forced-choice (2AFC) temporal order judgment (TOJ) on two extracted frames, identifying the earlier frame (15 trials). A 1-min retention interval preceded 20 additional TOJ trials without videoplay. Each day comprised four blocks with unique, unseen videos (8 clips each day). In addition, on Day 3, monkeys completed 120 TOJ trials integrating the full 16-clip set learned from preceding two days (*Top*). Recording chamber and sites (*Left*).

Single-Neuron Temporal Location Selectivity

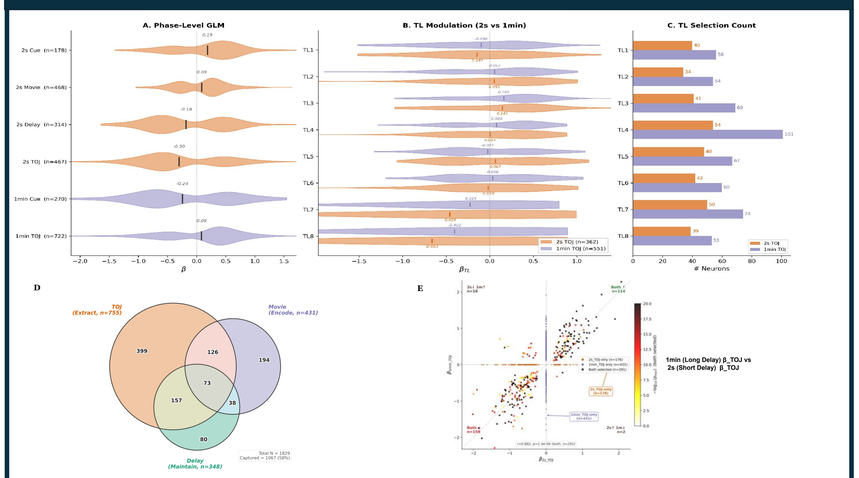

Fig. 2 Temporal location (TL) coding is distributed across task phases with correlated short- and long-delay modulation. Phase-level GLM β distributions (stepwise, 10 regressors). 1min_TOJ recruits more neurons (n=722) than 2s_TOJ (n=467); however, the two conditions show opposite polarity — 2s_TOJ is predominantly inhibitory (67% negative, mean β=−0.30), whereas 1min_TOJ is predominantly excitatory (64% positive, mean β=+0.09). (B) TL-level β split by delay condition. Latter TLs (TL7, TL8) show strongly negative modulation under both conditions (2s: −0.46, −0.66; 1min: −0.23, −0.40); early-to-mid TLs (TL2–TL4) carry positive modulation in both conditions. (C) TL selection counts. 1min_TOJ outnumbers 2s_TOJ at every TL, with TL4 showing the largest gap (101 vs. 54). (D) Venn diagram of phase selectivity across encoding (Movie), maintenance (Delay), and retrieval (TOJ) stages, showing substantial multi-phase overlap. (E) Modulation scatter of β_2s_TOJ vs β_1min_TOJ (N=898). Neurons (n=291) are strongly correlated (r=0.882, $p<10^{-96}$) across the two TOJ conditions, with the majority co-modulated in the same direction (Both↑=114, Both↓=159).

Neural Trajectories using PCA and Isomap show Subspaces

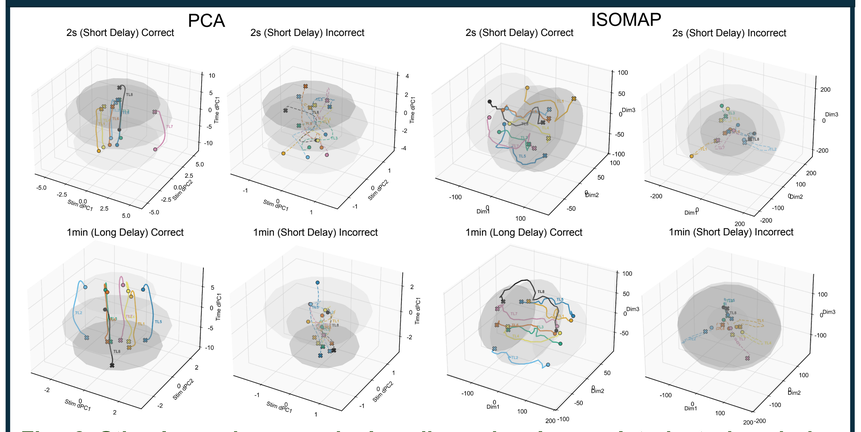

Fig. 3 Stimulus subspaces in low-dimensional neural trajectories during TOJ. A stimulus subspace being formed in the trajectories (by projecting population activity onto stimulus components) corresponding to different temporal locations (TLs), which is persistent throughout the TOJ period, for both short (2s, *Top*) and long (1 min, *Bottom*) delay, when the trajectories are visualized using either linear (PCA, *Left*) or non-linear (Isomap, *Right*) dimensionality-reduction methods. Such clear subspaces are seen for correct but *not* incorrect trials, where the trajectories for different TLs either do not move in tandem (PCA) or move randomly (Isomap). In addition, PCA trajectories for 1-min trials have a more strongly defined stimulus subspace across time, which flows smoothly and seems to expand around the middle of the TOJ period, but only for correct trials.

Dynamics of the Stimulus Subspace

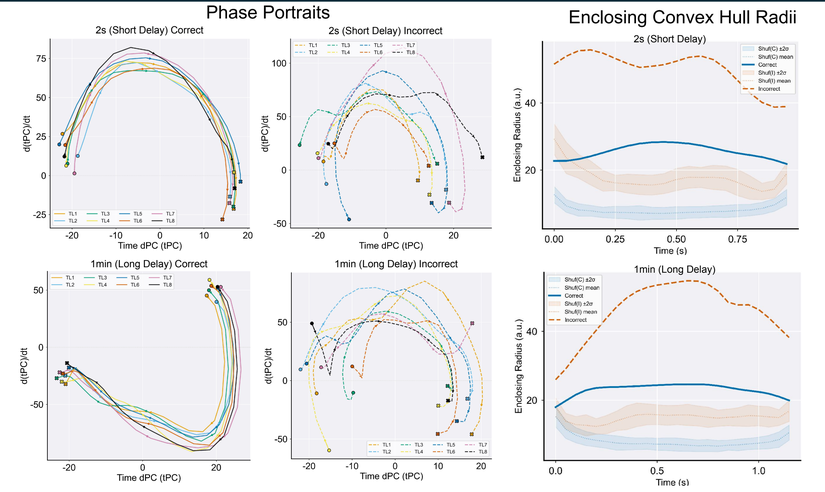

Fig. 4 The stimulus subspace is maintained persistently by synchronized trajectory dynamics in correct, but not incorrect trials during TOJ. Trajectory phase portraits, derived from plotting the temporal derivative of the primary time-related component (d(tPC)/dt) against its current state (tPC), for all 8 TLs are matched consistently for correct trials (*Left*), for both short (*Top*) and long (*Bottom*) delays – synchronous phase portraits create latent stimulus subspaces in correct trials. For incorrect trials (*Middle*), portraits are desynchronized. To quantify the size of the latent space varying with time, we also look at the radius of the convex hull which captures the trajectories for these spaces (*Right*). A latent space strongly emerges in the long delay and subsequently dissipates once the memory decision is reached. For the short delay, the latent space is maintained in memory for a longer duration. The bimodal distribution in trajectory speed suggests an evolving latent stimulus space, which settles into a larger size before gradually vanishing at the end of TOJ.

Topological Structure of Population Dynamics

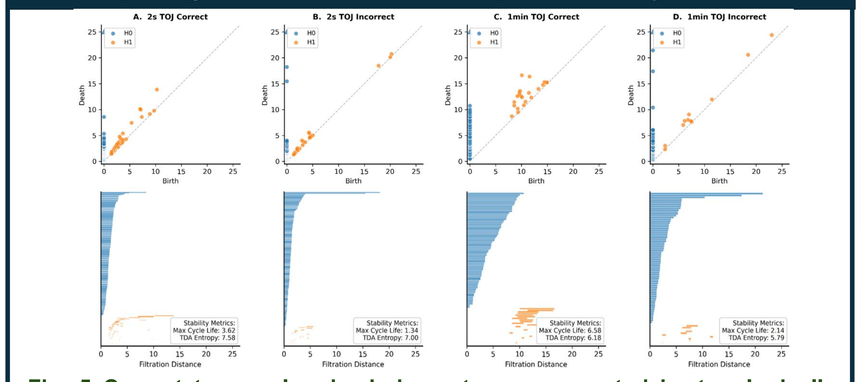

Fig. 5 Correct temporal order judgments are supported by topologically stable neural manifolds. (A–D) Persistence diagrams (Top) and barcodes (Bottom) for 2-s delay correct, 2-s delay incorrect, 1-min delay correct, and 1-min delay incorrect conditions. H_0 (blue): connected components; H_1 (orange): loops. Correct trials exhibit long-lived H_1 cycles far from the diagonal (Max Cycle Life: 3.62 short, 6.58 long), indicating persistent rotational structure (A, C). Incorrect trials show shorter-lived, fragmented features (Max Cycle Life: 1.34, 2.14) with lower TDA Entropy (7.00, 5.79 vs. 7.58, 6.18), reflecting a sparser manifold lacking coherent multi-scale organization (B, D).

Population Activity and Pair-Anchor Analysis Framework

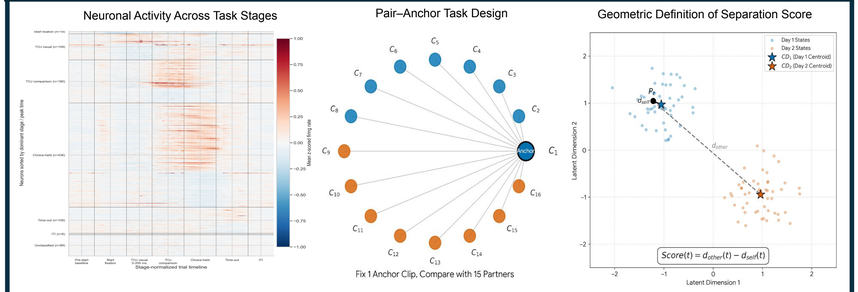

Fig. 6 Population activity and pair-anchor framework for quantifying day-specific separation. Stage-normalized population PSTH for Day 3 data (n=947), grouped by dominant stage and sorted by firing peak time (*Left*). Pair-Anchor Task Design. Schematic of analysis framework where neural trajectories are compared by fixing one clip as an Anchor and pairing it with 15 other Partner clips from Day 1 and Day 2 (*Middle*). Neural population activity was organized as a neurons × conditions × time tensor and projected into a dPCA subspace fitted within a cutoff window (-0.5 s to the shortest meanRT). Population activity was projected into a task-aligned dPCA subspace. For each point in each day-specific cluster, we compared their distance to the centroid of the other cluster (d_{other}) vs. to its own cluster (d_{own}) as a function of time (d_{other} (t) − d_{own} (t)) (*Right*).

Day-Specific Representational Geometry During Temporal Order Judgment

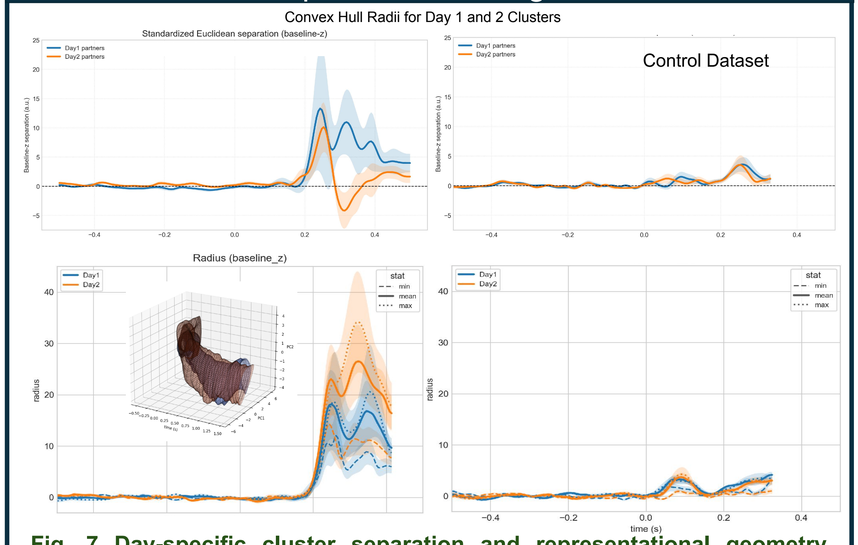

Fig. 7 Day-specific cluster separation and representational geometry emerge selectively during temporal order judgment on Day 3. A separation (computed as d_{other} (t) − d_{own} (t), see Fig. 6) between the day clusters is seen after onset of TOJ for the main experiment (*Top Left*), but not in control experiment (*Top Right*, n=450). Convex hulls enclosing day-specific clusters show that the more recent Day-2 cluster shows a clearly larger emergent radius, which corresponds to a higher representation volume of its hull (*Inset*) compared to Day-1, but only for the main dataset (*Bottom Left*), while such separation dynamics are not seen in the control dataset (*Bottom Right*). Hull radius was defined as centroid-to-boundary distance.

Conclusion

- The macaque precuneal neurons represent temporal locations through a unified computational framework. The shared modulation across scales suggests a stable neuronal axis for temporal indexing (Sarkar et al., 2026).
- The "manifold collapse" in error trials reveals the geometric basis of behavioral failure. The combination of centroid-based separation and convex-hull radius dynamics suggests that day-dependent retrieval context shapes episodic representations at multiple geometric levels.
- Memories of Day 1 and Day 2 events differ not only in where their trajectories are centered, but also in how their manifolds expand over time. Null effects in the control dataset suggest that these geometric differences reflect meaningful episodic organization.

References and Acknowledgments

- Clayton, N. S., & Dickinson, A. (1998). Episodic-like memory during cache recovery by scrub jays. *Nature*, *395*(6699), 272-274.
- Zuo, S., Wang, C., Wang, L., Jin, Z., Zhou, X., Su, N., ... & Kwok, S. C. (2026). Neural population dynamics and temporal context cells in macaque medial parietal cortex support temporal order memory. *PLoS biology*, *24*(4), e3003759.
- Sarkar, A., Wang, C., Zuo, S., & Howard, M. W. (2024). "What" x "When" working memory representations using Laplace Neural Manifolds. *arXiv preprint arXiv:2409.20484*

The work received support from the Kunshan Municipal Government research funding grant (24KKSGR017) and Duke University Provost Fund for Duke–DKU Collaborations (25KINTL013) (SCK).